Strain hardening in bidisperse polymer glasses: Separating the roles of chain orientation and interchain entanglement

Robert S. Hoy*

Materials Research Laboratory, University of California, Santa Barbara, CA 93106

Mark O. Robbins

Department of Physics and Astronomy, Johns Hopkins University, Baltimore, MD 21218
(Dated: November 24, 2018)

The effects of entanglement and chain orientation on strain hardening in glassy polymers are separated by examining mixtures of chains with different lengths. Simulations show that the orientation of a molecule of a given chain length is the same in monodisperse systems and bidisperse mixtures, even when entangled and unentangled chains are mixed. In addition, the stress in mixtures is equal to the weighted average of the stresses in monodisperse systems. These results indicate that chains contribute independently to strain hardening, that chain orientation is determined by local interactions with the surrounding glass, and that entanglements play at most an indirect role in strain hardening in the range of strains typically studied. We discuss these results in the context of recent microscopic theories.

PACS numbers: 61.41.+e,62.20.F-,81.40.Lm,83.10.Rs

I. INTRODUCTION

The mechanical performance and failure modes of glassy polymers are strongly affected by strain hardening; an increase in the stress needed to deform systems as the strain increases. There has been great interest in understanding the mechanisms of strain hardening so that it can be predicted and optimized for applications. Recent studies have challenged the traditional view that entanglements between polymer chains control strain hardening, and suggest that orientation of individual chains plays the dominant role. This paper uses simulations of polymer mixtures to separate the roles of entanglements and orientation.

The most widely used [1, 2] theories of strain hardening are based on rubber elasticity. They assume that entanglements between polymer chains act like chemical crosslinks in a rubber and that strain hardening arises from the decrease in entropy of an affinely deforming entanglement network [3]. The stress is written as

$$\sigma(\bar{\lambda}) \simeq \sigma_{flow} + G_R g(\bar{\lambda}) \quad (1)$$

where σ_{flow} is the plastic flow stress, G_R the "strain hardening modulus", $\bar{\lambda}$ the stretch tensor describing the macroscopic deformation, and g a dimensionless function that describes the reduction in chain entropy. This approach has had much success in fitting experimental stress strain curves, but the fits seem inconsistent with the underlying microscopic model [4]. One difficulty is that G_R is two orders of magnitude larger than expected near the glass transition temperature T_g. More troubling is that strain hardening grows with decreasing temperature, while any entropic force should decrease. A final

difficulty is that the theory does not explain the plastic flow stress, which must be added by hand.

A number of recent experiments and simulations have examined the origins of these difficulties [4, 5, 6, 7, 8, 9, 10, 11, 12, 13, 14, 15, 16, 17]. One realization is that the two terms on the right hand side of Eq. (1) are of similar magnitude and must arise from similar mechanisms. Experiment, theory and simulations all show that σ_{flow} and G_R are linearly related when pressure, T or strain rate is varied [10, 15, 16, 18]. This connection explains the large magnitude of G_R and the fact that it grows with decreasing temperature as is typical for the plastic flow stress. A direct connection between σ_{flow} and G_R has been established in the athermal limit $(T \to 0)$, where both contributions to the stress are given by a single scaling factor times the rate at which interchain bonds break during local plastic rearrangements [12, 13].

Simulations also show strain hardening occurs in polymers that are too short to form the entangled network that is assumed in rubber elasticity theories [12, 13, 14, 17]. Moreover, the strain hardening in these unentangled systems can be mapped to that of entangled chains if the macroscopic deformation $\bar{\lambda}$ in Eq. 1 is replaced [12, 13] by an effective stretch tensor $\bar{\lambda}_{eff}$ that describes the orientation of individual chains:

$$\sigma(\bar{\lambda}) = \sigma_{flow} + G_R^0 g(\bar{\lambda}_{eff}), \quad (2)$$

where G_R^0 is the value of G_R in the long-chain limit. The orientation of entangled chains is consistent with an affine deformation, $\bar{\lambda}_{eff} = \bar{\lambda}$. For unentangled systems the orientation is consistent with a subaffine deformation by $\bar{\lambda}_{eff}$.

The above findings support the notion that entanglements play an indirect role and that strain hardening is produced by the increased rate of local plastic rearrangements that are needed to maintain chain connectivity as

chains orient [12, 13, 19]. In contrast, other recent experiments [5, 20] suggest that entanglements play a central role. They find that G_R is directly proportional to the entanglement density ρ_e in both pure systems and polymer mixtures. However, there are other explanations for this correlation. For example, an increase in chain stiffness increases ρ_e and also stretches the chains so that more plastic rearrangements are required to maintain chain connectivity [13, 17, 21, 22].

In this paper we examine strain hardening of polymer mixtures. Using polymers with different chain lengths but the same interactions, stiffness, etc., allows us to isolate the roles of entanglements and orientation. The simulation results show that the orientation of chains plays the dominant role and that the response of mixtures has a surprisingly simple mean-field form. The variation of chain orientation with macroscopic stretch is nearly independent of the length of surrounding chains. In addition, the stress in mixtures is a simple weighted average of results for pure systems. These results suggest that strain hardening can be modeled as a sum of contributions from individual chains as they are deformed by interactions with the surrounding glass and produce local plastic rearrangements in the glass to maintain their connectivity.

II. POLYMER MODEL AND METHODS

Molecular dynamics (MD) simulations are performed using a coarse-grained bead-spring polymer model [23]. All monomers have mass m and interact via the truncated and shifted Lennard-Jones potential

$$U_{LJ}(r) = 4u_0[(a/r)^{12} - (a/r)^6 - (a/r_c)^{12} + (a/r_c)^6] \ , \ (3)$$

where $r_c = 1.5a$ is the cutoff radius and $U_{LJ}(r) = 0$ for $r > r_c$. Covalent bonds between adjacent monomers on a chain are modeled using the FENE potential

$$U(r) = -0.5kR_0^2 \ln(1 - (r/R_0)^2) \ , \qquad (4)$$

with the canonical [23] parameter choices $R_0 = 1.5a$ and $k = 30u_0/a^2$. The equilibrium covalent bond length is $l_0 = 0.96a$. We consider semiflexible chains with an angular potential $U_{bend} = k_{bend}(1 - cos(\theta))$, where θ is the angle between consecutive bond vectors along a chain. All quantities are expressed in units of the molecular diameter a, binding energy u_0, and characteristic time $\tau_{LJ} = \sqrt{ma^2/u_0}$. Periodic boundary conditions are imposed, with periods L_i along directions $i = x$, y, and z.

Simulations are performed using the same protocols as in Refs. [11, 12, 13]. A rapid quench is applied to well-equilibrated melts [24], producing glasses at the desired temperature T. The rapidity of the quench suppresses aging and strain softening. The simulations presented here are performed at $T = 0.2u_0/k_B$ and $T = 0.275u_0/k_B$. Both values are well below the glass transition temperature $T_g \simeq u_0/3k_B$ [25], yet sufficiently high

to observe significant thermally-activated rate-dependent relaxation [11]. Uniaxial compression is performed at constant strain rate $\dot{\epsilon} \equiv \dot{L}_z/L_z$. The volume stays nearly constant during compression. In this case the function describing the entropy loss in Eq. 1 can be written as $g(\lambda) = 1/\lambda^2 - \lambda$ where $\lambda = L_z/L_z^0$ is the stretch relative to the initial size L_{z0}.

The strain rates used range from $10^{-6}/\tau_{LJ}$ to $10^{-4}/\tau_{LJ}$. While these rates are higher than experiment, previous studies in this range of $\dot{\epsilon}$ and T have been shown to capture many aspects of experiments, including logarithmic rate dependence [25], creep [26], and a linear relationship between flow and hardening modulus [15]. Our rates are also orders of magnitude slower than those obtainable with more computationally intensive united atom models (e. g. Ref. [17]). At the higher rates studied with these potentials, unentangled chains deform nearly affinely because there is insufficient time for activated motion of chains relative to their neighbors. This motion is particularly important for the chain length dependence of strain hardening considered here.

Systems contain short and long chains with N_{short} and N_{long} monomers, respectively. The total number of monomers is N_{tot} and the weight fraction of short chains is f. We present results for $N_{long} = 350$, $10 \leq N_{short} \leq 25$, and $k_{bend} = 0.75\epsilon$, but equivalent results were obtained for a range of other values. For this k_{bend}, the entanglement length is $N_e \sim 40$ monomers [27]. In experiments, unentangled glasses with $N \lesssim N_e$ typically exhibit brittle fracture, but fracture is suppressed in simulations [11, 14], perhaps because of the small system size and periodic boundary conditions.

III. RESULTS

Panels (a) and (b) of Figure 1 show the stress as a function of $g(\lambda)$ for mixtures with $N_{short} = 10$ and 25, respectively. Results for $f = 0.5$ lie directly between the results for pure systems with $f = 0$ and 1. Also shown is the weighted average of the pure system results

$$\sigma_{ave} = (1 - f)\sigma_{long} + f\sigma_{short} \qquad (5)$$

for $f = 0.5$. Within our statistical accuracy, the stress in the mixtures is equal to this weighted average. We have verified that this "stress superposition principle" holds for different k_{bend}, chain lengths, temperatures and f. The only discrepancies are observed at large g (> 3.5) when chains in entangled systems have stretched nearly taut and significant energy is stored in the covalent bonds. Experiments only reach such large stretches when special sample preparation procedures are used [2, 29].

Equation (1) would predict a linear increase in stress with g. The systems in Fig. 1 were chosen to exhibit deviations from this straight line behavior, but still obey stress superposition. Deviations from linearity in experiments are often fit by including non-Gaussian (finite chain length) corrections to the network entropy
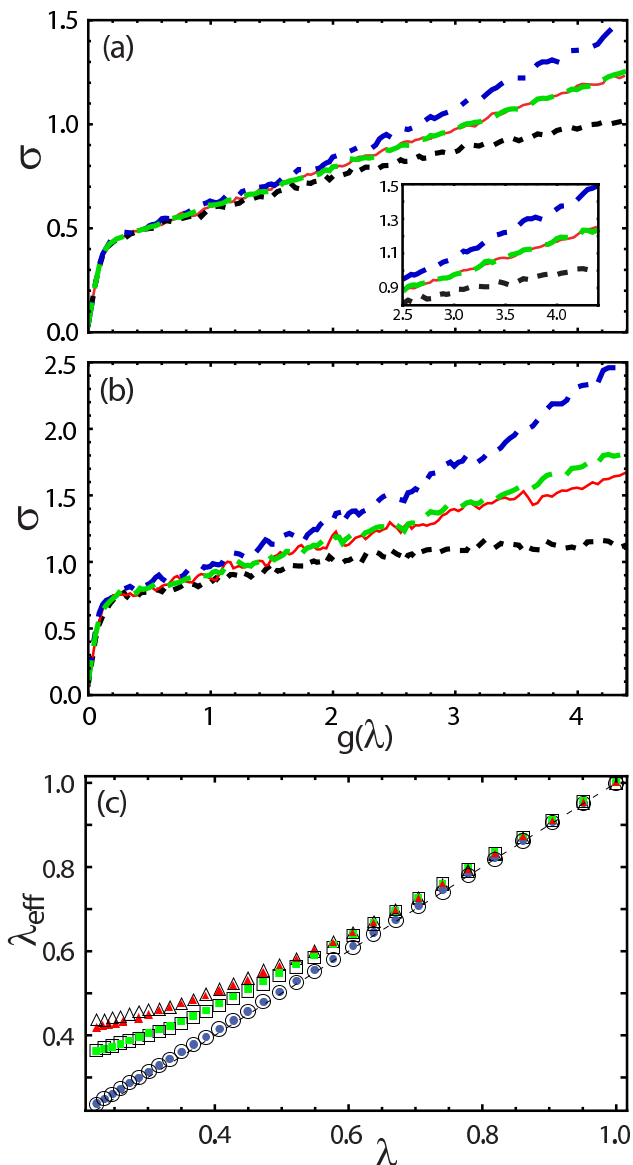
FIG. 1: Panels (a-b): Stress plotted against $g(\lambda)$ for uniaxial compression of monodisperse glasses with length N_{long} (dash-dotted) or N_{short} (dotted) and of 50/50 mixtures of the two lengths (dashed). The solid curves show the average of the two monodisperse systems. Here $k_{bend} = 0.75$ ($N_e = 39$). Panel (a): $N_{short} = 25$, $T = .275u_0/k_B$ and $|\dot{\epsilon}| = 10^{-5}/\tau_{LJ}$. The inset shows a blowup of the data at large g [28]. Panel (b): $N_{short} = 10$, $T = 0.2u_0/k_B$ and $|\dot{\epsilon}| = 10^{-4}/\tau_{LJ}$. Panel (c): Variation of λ_{eff} with λ for pure systems with $N = 350$ (solid circles), $N = 25$ (solid squares), and $N = 10$ (solid triangles). Open symbols of the same shape show results for chains of each length in $f = 0.5$ mixtures.

[2]. Previous simulations are not consistent with this interpretation [12, 13]. They show that the upturn in stress for entangled systems reflects energy stored in the glass, while the downward curvature for unentangled systems results from subaffine deformation of the chains ($|ln(\lambda_{eff}))| < |ln(\lambda)|$). Despite the different curvatures

for the long and short chains in Fig. 1 their contributions to the stress in mixtures are simply additive.

These results do not conflict with experiments that found G_R was proportional to ρ_e [5, 30]. For the specific polymers studied, the entanglement density of mixtures is a weighted average of pure systems. Thus these systems also obey stress superposition. It would be interesting to perform similar experiments on polymer mixtures whose entanglement density was a nonlinear function of weight fraction.

The relation between ρ_e and f is nonlinear for the model polymers considered here, yet plots in a previous paper indicated G_R was proportional to ρ_e [11]. While this is approximately true for monodisperse systems, the results for mixtures were misinterpreted in this earlier paper. A factor of $(1 - f)$ was inadvertently excluded in the calculation [31] of ρ_e from Primitive Path Analysis [27]. When ρ_e is evaluated correctly, the hardening modulus is no longer proportional to ρ_e. However, we do find that the values of G_r from Ref. [11] satisfy stress superposition. Indeed, the superposition principle explains the success of the previous collapse. As noted in Ref. [11], the incorrectly determined value of ρ_e was proportional to $(1 - f)$ and so the collapse implied $G_R \propto (1 - f)$ as expected from superposition. The correct ρ_e is nearly proportional to $(1 - f)^2$ and not linearly related to G_R.

To understand why the contribution of chains to stress is additive, we examined the changes in molecular conformations during shear. As in Ref. [12], the orientation was quantified by the effective stretch λ_{eff}. This is defined as the mean stretch of chains along the compression direction; $\lambda_{eff} = \langle R_z/R_z^0 \rangle$, where R_z is the rms z-component of the end-to-end vector of a chain and R_z^0 the value before strain. Panel (c) shows $\lambda_{eff}(\lambda)$ for short and long chains in the pure and mixed states for the same systems shown in panels (a-b). Remarkably, λ_{eff}^{long} and λ_{eff}^{short} do not themselves depend on f. In other words, the orientation of the long (short) chains is not dependent on whether they are in a pure system or mixed with a fairly high fraction of short (long) chains. This f-independence of λ_{eff} holds over the same broad range of conditions as the stress superposition principle.

How can we understand the apparent f-independence of λ_{eff}? The simplest qualitative picture is that inter-chain interactions in the glass tend to enforce an affine deformation of the chains, but that this is opposed by intrachain bonds. Chains can not deform affinely at small scales because this would stretch the stiff covalent bonds along the chains. Instead, chains are observed to straighten over an effective persistence length l_p that increases with g [11, 17]. This straightening is independent of chain length until the associated stress becomes large enough to force relaxation of the chain along its length. For the systems considered here, the friction with neighboring chains is large enough that significant relaxation does not occur until unentangled chains are stretched to a substantial fraction of their fully extended length. Straightening chains while maintaining their con-

nectivity requires local rearrangements of the surrounding monomers. The number of rearrangements grows with the persistence length and this was found to correlate directly with the strain hardening at low temperatures [12, 13, 17, 21].

Note that entanglements do not enter directly in this picture. Since entangled and unentangled chains behave in the same manner at small $|g|$, the constraints on their rearrangements must be determined by very local interactions with the surrounding matrix. Entanglements only become relevant when g is so large that l_p reaches a significant fraction of the separation between entanglements [12, 13]. In this limit entanglements become more effective than friction from the matrix in enforcing an affine displacement of the chain. The associated tension in the chains grows as l_p approaches $N_e l_0$ and contributes significant energetic terms to the strain hardening at large $|g|$ [13, 29, 32, 33].

It is worth considering under which conditions this mean field picture should break down. For the reasons just described, the range of validity will be limited to small strains in very densely entangled systems; fortunately, by this standard, few synthetic polymers are so densely entangled [34]. The mean field picture should also break down for extremely short chains where the high density of chain ends changes the density, friction and other properties significantly. Stress superposition will be particularly sensitive to changes in the relaxation rate of chains on the end-end scale, τ_{relax}^{-1}, with f. These are known to be significant for T above T_g, where τ_{relax} for short chains is increased when they are mixed with longer chains, leading to greater orientation at a given shear rate [35, 36]. Our results show that such coupled-orientation effects are small deep in the glassy state.

IV. DISCUSSION AND CONCLUSIONS

The simulations presented here provide further evidence that strain hardening in polymer glasses depends primarily on chain orientation rather than entanglement. They also provide new insight into the factors that control the degree of orientation. The local coupling to the glassy matrix enforces an affine deformation of the chains ($\lambda = \lambda_{eff}$) at small $|g|$. Hardening arises primarily from the plastic rearrangements needed to maintain intrachain connectivity as chains orient and are straightened over greater lengths. As the associated stress on the chains grows, there is an increasing tendency for them to relax along their length, leading to subaffine deformation ($\lambda \neq \lambda_{eff}$). The observation that the value of λ_{eff} for a given chain length is independent of f and that the

stress due to plastic rearrangements obeys the superposition principle, implies that chains relax nearly independently. The degree of relaxation depends on a competition between the intrachain tension caused by alignment and friction with the glassy matrix. Entanglements only enter at very large $|g|$ where they prevent relaxation of chains that are much longer than N_e.

To our knowledge, no microscopic theory that predicts the functional form of λ_{eff} in glasses has been published. Constitutive models which employ a viscoelastic or viscoplastic description of glassy strain hardening (e. g. Refs. [37, 38, 39]) typically decompose $\bar{\lambda}$ into rubber-elastic and plastic parts (or use other internal state variables), but do not explicitly account for $\lambda \neq \lambda_{eff}$ or the N-dependence of nonaffine relaxation [40]. It would be interesting to see if a first principles theory like that of Ref. [18] could be generalized to predict $\lambda_{eff}(\lambda)$. The qualitative ingredients that must enter such a microscopic theory are evident from the results shown here and in Refs. [12, 13, 17]. Simply put, λ_{eff} falls behind λ when the stress in the material is insufficient to further affinely orient the average chain.

Fortuitously, λ_{eff} can now be accurately measured in scanning near-field optical microscopy experiments [41] which can discriminate values for different chain lengths in a bidisperse system. Ref. [41] showed λ_{eff} falls behind λ for entangled chains deformed slightly above T_g; similar studies on a variety of chain lengths below T_g would be of great interest. These might prove that λ_{eff} is one of the "mesoscale" quantities [42] whose understanding will improve modeling of the deformation of amorphous materials. Other recent experiments [43] have shown that segmental dynamics and larger-scale polymer dynamics are nontrivially coupled below T_g. Further developments along these lines would be welcome, as would extension of the recently improved understanding of the relation [44] between linear viscoelastic behavior and structural relaxation to the nonlinear regime.

[1] R. N. Haward and G. Thackray, Proc. Roy. Soc. Lond. **302**, 453 (1968).

[2] E. M. Arruda and M. C. Boyce, Int. J. Plast. **9**, 697 (1993).

[3] Hereon tensor notation for $\bar{\lambda}$ is dropped for convenience, but λ and λ_{eff} remain tensorial.

[4] E. J. Kramer, J. Polym. Sci. Part B - Polym. Phys. **43**, 3369 (2005).

[5] H. G. H. van Melick, L. E. Govaert, and H. E. H. Meijer, Polymer **44**, 2493 (2003).

[6] R. B. Dupaix and M. C. Boyce, Polymer **46**, 4827 (2005).

[7] M. Wendlandt, T. A. Tervoort, and U. W. Suter, Polymer **46**, 11786 (2005). M. Wendlandt, T. A. Tervoort, J. D. van Beek, and U. W. Suter, J. Mech. Phys. Solids **54**, 589 (2006).

[8] P. J. Hine, A. Duckett, and D. J. Read, Macromolecules **40**, 2782 (2007).

[9] F. Casas, C. Alba-Simionesco, H. Montes, and F. Lequeux, Macromolecules **41**, 860 (2008).

[10] L. E. Govaert, T. A. P. Engels, M. Wendlandt, T. T. A, and U. W. Suter, J. Polym. Sci. Part B - Polym. Phys. **46**, 2475 (2008).

[11] R. S. Hoy and M. O. Robbins, J. Polym. Sci. Part B - Polymer Phys. **44**, 3487 (2006).

[12] R. S. Hoy and M. O. Robbins, Phys. Rev. Lett. **99**, 117801 (2007).

[13] R. S. Hoy and M. O. Robbins, Phys. Rev. E **77**, 031801 (2008).

[14] A. V. Lyulin, N. K. Balabaev, M. A. Mazo, and M. A. J. Michels, Macromolecules **37**, 8785 (2004); A. V. Lyulin, B. Vorselaars, M. A. Mazo, N. K. Balabaev, and M. A. J. Michels, Europhys. Lett, **71**, 618 (2005).

[15] M. O. Robbins and R. S. Hoy, J. Polym. Sci. Part B - Polym. Phys. **47**, 1406 (2009).

[16] B. Vorselaars, A. V. Lyulin, and M. A. J. Michels, J. Chem. Phys. **130**, 074905 (2009).

[17] B. Vorselaars, A. V. Lyulin, and M. A. J. Michels, Macromolecules **42**, 5829 (2009).

[18] K. Chen and K. S. Schweizer, Phys. Rev. Lett **102**, 038301 (2009).

[19] A. S. Argon, Philos. Mag. **28**, 39 (1973).

[20] C. G'Sell and A. Souahi, J. Eng. Materials Tech. **119**, 223 (1997).

[21] J. I. Mckechnie, R. N. Haward, D. Brown, and J. H. R. Clarke, Macromolecules **26**, 198 (1993).

[22] L. J. Fetters, D. J. Lohse, D. Richter, T. A. Witten, and A. Zirkel, Macromolecules **27**, 4639 (1994).

[23] K. Kremer and G. S. Grest, J. Chem. Phys. **92**, 5057 (1990).

[24] R. Auhl, R. Everarers, G. S. Grest, K. Kremer, and S. J. Plimpton, J. Chem. Phys. **119**, 12718 (2003).

[25] J. Rottler and M. O. Robbins, Phys. Rev. E **68**, 011507 (2003).

[26] M. Warren and J. Rottler, Phys. Rev. E **76**, 031802 (2007); R. A. Riggleman, K. S. Schweizer, and J. J. de Pablo, Macromolecules **41**, 4969 (2008).

[27] R. Everaers, S. K. Sukumaran, G. S. Grest, C. Svaneborg, A. Sivasubramanian, and K. Kremer, Science **303**, 823 (2004).

[28] A smaller system with the same parameters as in panel (a) was tested at $|\dot{\epsilon}| = 10^{-6}/\tau_{LJ}$ and gave equivalent results, but these were noisier due to finite size effects. Changing the rate by two orders of magnitude had only a modest effect on λ_{eff}, as expected from a logarithmic rate sensitivity.

[29] O. A. Hasan and M. C. Boyce, Polymer **34**, 5085 (1993).

[30] Z. Bartczak, Macromolecules **38**, 7702 (2005).

[31] We thank Alexei E. Likhtman and Daniel J. Read for pointing out an inconsistency that led to this discovery.

[32] C. Chui and M. C. Boyce, Macromolecules **32**, 3795 (1999).

[33] J. Li, T. Mulder, B. Vorselaars, A. V. Lyulin, and M. A. . J. Michels, Macromolecules **39**, 7774 (2006).

[34] R. N. Haward, Macromolecules **26**, 5860 (1993).

[35] A. R. C. Baljon, G. S. Grest, and T. A. Witten, Macromolecules **28**, 1835 (1995).

[36] C. M. Ylitalo, J. A. Kornfield, G. G. Fuller, and D. S. Pearson, Macromolecules **24**, 749 (1991).

[37] L. Anand and M. E. Gurtin, Int. J. Solids Structures **40**, 1465 (2003).

[38] J. M. Caruthers, D. B. Adolf, R. S. Chambers, and P. Shrikhande, Polymer **45**, 4577 (2004).

[39] R. B. Dupaix and M. C. Boyce, Mech. Materials **39**, 39 (2007).

[40] Ref. [46] considered N-dependent (reptational) relaxation of incompletely crosslinked elastomers above T_g and it would be interesting to see if this approach could be adapted to glassy systems.

[41] T. Ube, H. Aoki, S. Ito, J. Horinaka, and T. Takigawa, Polymer **48**, 6221 (2007); T. Ube, H. Aoki, S. Ito, J. Horinaka, T. Takigawa, and T. Masuda, Polymer **50**, 3016 (2009).

[42] J. Barrat and J. J. de Pablo, MRS Bull. **32**, 941 (2007).

[43] J. Hintermeyer, A. Herrmann, R. Kahlau, C. Goiceanu, and E. A. Rössler, Macromolecules **41**, 9335 (2008).

[44] L. Grassia and A. D'Amore, J. Polym. Sci. Part B - Polym. Phys. **47**, 724 (2009).

[45] http://lammps.sandia.gov/.

[46] J. S. Bergström and M. C. Boyce, J. Mech. Phys. Solids **46**, 931 (1998).